Phase synchronization in a heat bath and the lattice dynamics of metals under Fermi-resonance conditions

Yu. N. Gornostyrev and M. I. Katsnel'son

Institute of the Physics of Metals, 620219 Ekaterinburg, Russia

A. P. Platonov and A. V. Trefilov

Kurchatov Institute, 123182 Moscow, Russia

(Submitted 13 October 1994)
Zh. Éksp. Teor. Fiz. **107**, 925–935 (March 1995)

Phase synchronization in a system of interacting nonlinear oscillators with a frequency ratio of 1:2 in the presence of white noise, simulating the interaction of the phases with a heat bath, was investigated by means of computer modeling. It was shown that phase synchronization exists over a wide range of model parameters, and when the intensity of the fluctuations (i.e., the temperature) or the nonlinear coupling constant increase sufficiently, a transition to chaos occurs. The classical Fermi-resonance regime was investigated, and the application of the results obtained to specific metals is briefly discussed. © *1995 American Institute of Physics.*

1. INTRODUCTION

The ideas and methods of the modern theory of dynamical systems are successfully applied in the most diverse fields of physics, and they are making it possible to establish deep structural analogies between seemingly disparate physical phenomena.[1–3] At the same time, the "nonlinear ideology" is virtually never used to study the dynamics of crystal lattices, apart from the simplest phenomena, such as the amplitude dependence of the frequency of an anharmonic oscillator, giving rise to thermal expansion, or scattering of weakly interacting waves, which determines, for example, the thermal conductivity of crystals (see, for example, Ref. 4). This situation is probably explained by the fact that in many important problems, for example in the study of the thermodynamics of crystals, the standard anharmonic perturbation theory is well-founded (because of the presence of a small adiabaticity parameter κ) and effective.[5,6] As noted in Refs. 7 and 8, however, in calculations of the dynamic structure factor measured in inelastic neutron scattering experiments, this theory can be inadequate even if $\kappa \ll 1$ because of the fact that subtle phase relations between the interacting phonons are neglected. A similar situation occurs in the theory of disordered systems, where the key phenomenon—Anderson localization—cannot be studied by the average Green's function method, once again because averaging destroys information about the phase of the wave function.[9]

An example of a nonlinear phenomenon that is sensitive to the phase relations and cannot be described in the standard phonon language is phase synchronization with a rational ratio of the seed frequencies of the phonons from different branches of the spectrum for definite values of the quasimomentum.[8,10] These results are only preliminary indications, however, since in our preceding works[7,8,10] the scales and the specific conditions under which this phenomenon appears were not estimated as a function of the model parameters. A systematic solution of these problems requires that the effect of thermal fluctuations on the dynamical system (two coupled nonlinear oscillators) be taken into account, and this is our objective in the present paper. Here, phase synchronization is studied by direct numerical modeling of this phenomenon in a heat bath simulated by white noise. At the same time, the question of the manifestation of the phase synchronization of actually observed quantities (in experiments on quasielastic and inelastic neutron scattering) has been adequately studied in Ref. 10 and will not be discussed here. The results of the present investigation could be of much more general interest than the specific problem formulated above, since the phase synchronization phenomenon is encountered in the most diverse physics and engineering systems,[1,2,11] and the effect of random perturbations on this phenomenon has essentially never been studied.

2. FORMULATION OF THE MODEL

Consider a system of two coupled oscillators described by the Lagrangian

$$L=\tfrac{1}{2}(\dot{u}^2+\dot{v}^2)-\tfrac{1}{2}\omega_0^2u^2-\tfrac{1}{2}\Omega_0^2v^2-\lambda uv^2-\sigma(u^4+v^4), \tag{1}$$

where $u(t)$ and $v(t)$ are the coordinates of the oscillator, ω_0 and Ω_0 are the frequencies of small oscillations and are in the ratio 2:1 ($\omega_0=2\Omega_0+\nu$, $|\nu|\ll\omega$), λ is the anharmonic coupling constant responsible for phase synchronization, and "intramode" anharmonicity terms proportional to σ are included in order to guarantee stable motion for large values of u and v ($\sigma>0$).

This model is probably the simplest model that describes phase synchronization (the well-known "spring pendulum" model of Vitt and Gorelik[12] also contains anharmonic terms in the kinetic energy). Similar systems were apparently first studied in connection with the so-called Fermi resonance problem[13–15]—singularities of the infrared and Raman spectra of molecules with a rational ratio of the frequencies [for example, 1:2 in the case of CO_2 (Ref. 13)]. For molecules, however, the ultraquantum limit $\omega \gg T$ (T is the temperature) is valid;[14] this case is much simpler than the classical case studied here, when ω is at most of order T. As we shall see

 1063-7761/95/030525-06$10.00

below, the latter case is of interest for metals. In the ultraquantum limit the Fermi resonance results in splitting of a series of lines and violation of the selection rules that forbid certain lines in the Raman scattering spectra.[15] In the classical regime, however, as we shall see, the picture is much richer; a low-frequency component appears in the spectrum,[7,8,10] a transition to chaos can occur, and so on. The onset of low-frequency dynamics is especially interesting; roughly speaking, this dynamics relates to the Fermi resonance as electron paramagnetic resonance (microwave transition between Zeeman sublevels) relates to the Zeeman effect (splitting of optical lines). In the ultraquantum limit, the intensity of these low-frequency transitions is of the order of $\exp(-\omega_0/T)$, i.e., it is vanishingly small.[7]

Adding damping and random forces to the equations of motion with the Lagrangian (1) gives

$$\begin{aligned}&\ddot{u}+2\gamma\dot{u}+\omega_0^2u+\lambda v^2+4\sigma u^3=f_u(t),\\&\ddot{v}+2\Gamma\dot{v}+\Omega_0^2v+2\lambda uv+4\sigma v^3=f_v(t),\end{aligned}\tag{2}$$

where γ and Γ are the corresponding damping constants of the oscillations and f_i are random forces of the "white noise" type with the correlation functions

$$\langle f_u(t)f_u(t')\rangle=4T\gamma\delta(t-t'),$$

$$\langle f_v(t)f_v(t')\rangle=4T\Gamma\delta(t-t'),\quad \langle f_u(t)f_v(t')\rangle=0.$$

It is well known that this choice of correlation functions guarantees that the system will relax to a Gibbs distribution corresponding to the temperature T.[16] The system of equations (2) gives an approximate description of the transverse and longitudinal phonons at the point

$$\mathbf{q}_0=\frac{2\pi}{a}\left(\frac{2}{3},\frac{2}{3},\frac{2}{3}\right)$$

of metals with a body-centered cubic lattice (a is the lattice parameter). It differs from the model studied in Ref. 10 in that it includes random forces and terms with σ. To better represent the real values of the parameters, we present the results of microscopic calculations for potassium at constant temperature:[10]

ω_0	Ω_0	Γ	γ	T	λ
0.55	0.275	0.040	0.027	0.015	0.050

(3)

Here, the frequencies and damping are given in units of the ion plasma frequency ω_{pi}, T is given in units of $M\omega_{pi}^2(a/2\pi)^2$, and λ is given in units of $M\omega_{pi}^2(2\pi/a)$.

In the numerical calculations the parameters ω_0, Ω_0, and λ were chosen near these values, and γ and Γ were varied in proportion to T, as should be for phonon damping at temperatures above the Debye temperature.[6] A reasonable estimate for σ, ensuring that the corresponding contribution to the total energy is small for the thermodynamic equilibrium values

$$u_T=\sqrt{(T/\omega_0^2)},\quad v_T=\sqrt{(T/\Omega_0^2)},$$

is $\sigma=0.004$–0.008. In most cases we set $\sigma=0.0055$. To speed the thermalization process, the initial conditions were chosen in the form $u=u_T$, $v=v_T$, $\dot{u}=0$, and $\dot{v}=0$.

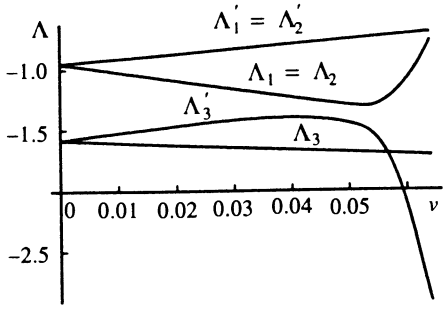

FIG. 1. Eigenvalues of the matrix M_{ij}, which determines the stability of two fixed points (primed and unprimed, respectively), as a function of the detuning of the frequency ν for the parameter values given in (3).

3. INVESTIGATION OF PHASE SYNCHRONIZATION IN A SIMPLIFIED MODEL

To understand the possible regimes of behavior of the system (2), we shall analyze first a simplified version of this model. For this, we represent the solution in the form

$$u(t)=2\mathrm{Re}[A(t)\exp(-i\omega_0t)],$$

$$v(t)=\mathrm{Re}[C(t)\exp(i\omega_0t/2)],$$

and where $A=r\exp(i\phi_1)$ and $C=R\exp(i\phi_2)$ are complex amplitudes, which change over a time interval of the order of λ^{-1}. Neglecting the rapidly oscillating terms in the equations for A and C as well as the terms which are of higher order in λ, we transform the system (2) to the form

$$\begin{aligned}&\frac{\partial r}{\partial t}+\gamma(r-u_T)+\frac{\lambda}{2\omega_0}R^2\sin\Phi=0,\\&\frac{\partial R}{\partial t}+\Gamma(R-v_T)-\frac{2\lambda}{\omega_0}Rr\sin\Phi=0,\\&\frac{\partial\Phi}{\partial t}+\nu+\frac{\lambda}{2\omega_0}\left(\frac{R^2}{r}-8r\right)\cos\Phi=0,\end{aligned}\tag{4}$$

where $\Phi=\phi_1+2\phi_2$. The interaction with the heat bath is taken into account in Eqs. (4) by introducing the terms $-\gamma u_T$ and $-\Gamma v_T$, which describe the relaxation of r and R to the thermodynamic equilibrium values. This system of equations was derived in Ref. 10. Here we give the results of its numerical solution.

Phase synchronization, i.e., the regime with $\Phi=$const and a definite ratio of r and R, corresponds to stable fixed points of the system of equations (4). The fixed point (r^*, R^*, Φ^*) is stable is all eigenvalues Λ_i of the matrix $\|M_{ij}\|$ in the linearized equation

$$\dot{a}_i=\Sigma_jM_{ij}a_i$$

[$\mathbf{a}=(r,R,\Phi)$] have a negative real part. A numerical investigation for the parameters (3) showed that for $\nu\leqslant\nu_c\approx0.065$ there exist two such points, and the initial conditions determine the point to which the solution of Eq. 4 is attracted. Indeed, one can see from Fig. 1 that $\Lambda_i<0$ for all ν for which solutions exist for a fixed point. Figure 2 displays the approach of the solutions $\Phi(t)$ of Eqs. (4) to a fixed point under different initial con-

ditions. For $\nu > \nu_c$ there are no fixed points. For what follows, it is important that, first, two fixed points exist and, second, phase synchronization remains over a wide range of detunings ν/ω_0, of the order of 12%. Over this entire interval, one fixed point of Φ lies close to 0 and another lies close to π (0.031π and 0.97π with $\nu=0$).

4. NUMERICAL MODELING PROCEDURE

The system of equations (2) was solved by integrating the stochastic equations directly by a standard method.[17] This method is an extension of the Runge–Kutta scheme used for solving deterministic differential equations. In the latter case, the desired solution $x(t+h)$ is constructed by expanding in powers of the step h, such that the order of magnitude of the error not exceed h^k, where k is the order of the method. In application to stochastic differential equations, this procedure is modified: in addition to the standard Taylor part, there appears an expansion in powers of $\sqrt{h}$ for the random Wiener process. An algorithm of order k is a procedure for which the error of all moments of the random function $x(t+h)-x(t)$ does not exceed h^k.

In application to the solution of a system of differential equations of the form

$$\frac{d\mathbf{x}}{dt}=\mathbf{f}(\mathbf{x})+\mathbf{A}(t)\ , \tag{5}$$

where

$$\langle A_k(t)\rangle=0,$$

$$\langle A_k(t)A_\mu(t')\rangle=\xi_k\delta_{k\mu}\delta(t-t'),$$

$k=1,\ldots,N$, and N is the number of equations, the corresponding l-step numerical algorithm is as follows:[17]

$$\begin{aligned}
g_{1k}&=f_k(\{x_{0\mu}+\sqrt{h}\sqrt{\xi_\mu}Y_{1\mu}\}),\\
g_{2k}&=f_k(\{x_{0\mu}+h\beta_{21}g_{1\mu}+\sqrt{h}\sqrt{\xi_\mu}Y_{2\mu}\}\\
g_{lk}&=f_k(\{x_{0\mu}+h\beta_{l1}g_{1\mu}+\ldots+h\beta_{l,l-1}g_{l-1\mu}+\sqrt{h}\sqrt{\xi_\mu}Y_{l\mu}\},\\
x_k(h)&=x_{0k}+h(A_1g_{1k}+\ldots+A_lg_{lk})+\sqrt{h}\sqrt{\xi_\mu}Y_{0\mu}.
\end{aligned} \tag{6}$$

Here, $\{x_\mu\}$ is the set of variables $x_1,\ldots,x_N$, and Y_{ik} is a random quantity with covariance

$$\langle Y_{ik}Y_{j\mu}\rangle=L_{ij}\delta_{k\mu}\ , \tag{7}$$

or, equivalently,

$$Y_{ik}=\sum_{j=1}^{m}\lambda_{ij}Z_{jk}\ , \tag{8}$$

where Z_{ik} are Nm independent Gaussian random variables with zero mean and unit variance. Generally speaking, $m=l+1$, but in certain cases an algorithm can also be constructed with a smaller value of m.

We employed a four-step third-order method, designated in Ref. 17 as $3_O4_S2_G$ with $m=2$ and the parameters A_i, β_{ij}, and λ_{ij} presented in Ref. 17. This method was previously found to be helpful in modeling anomalous lattice dynamics in strongly anharmonic crystals (in the much simpler case of one mode).[18] The system of equations (2) was integrated over a sequence of time intervals $[t_I,\ t_{I+1}]$ of the same length $t'=t_{I+1}-t_I$, and the state of the system reached by the end of the Ith interval was taken as the initial state for the next segment. To find the frequency spectrum, corresponding to a long-time realization $x(t)$ of length Mt' ($M\gg 1$; x is u, v, or uv^2), the coefficients $a_I(\omega_n)$ of the discrete Fourier transform were determined for each Ith time interval,

$$a_{(I)}(\omega_n)=\Delta t\sum_{j=1}^{m-1}x(t_{IJ})\exp(-i\omega_n j\Delta t) \tag{9}$$

and then summed with the weight $\exp(-i\omega_n t_I)$

$$a(\omega_n)=\sum_{I=0}^{M}a_I(\omega_n)\exp(-i\omega_n t_I). \tag{10}$$

Here, m is the number of partition points, $\Delta t=t'/(m-1)$, the times t_j lie in the interval $[t_I,\ t_{I+1}]$, and $t_I=It'$. To calculate the Fourier transform, the realization $x(t)$ was replaced by $x(t)-\bar{x}$, where $\bar{x}$ is the average displacement over the integration time. As a result, a contribution from static displacements of the type $\bar{x}^2\delta(\omega)$ was eliminated from the spectral density $P(\omega)=|a(\omega)|^2$.

To estimate the power spectrum $P(\omega)$, a well-defined procedure must be used for filtering (smoothing) the computed periodogram $\tilde{P}(\omega_n)$. Such a procedure, on the one hand, makes it possible to eliminate unphysical oscillations resulting from the computational error and, on the other hand, to simulate the Gaussian instrumental broadening in the experimental determination of $P(\omega)$, for example, by means of neutron scattering. We employed the filtering procedure described in Ref. 19 in which the power spectrum is estimated by the expression

$$P(\omega)=\frac{1}{\sqrt{2\pi}s}\int_{-\infty}^{\infty}\tilde{P}(\omega')\exp\left(-\frac{(\omega-\omega')^2}{2s^2}\right)d\omega'. \tag{11}$$

We used Simpson's rule to integrate over a discrete set of points trapezoidal method. The quantity s was set equal to $1.5\Delta\omega$, where $\Delta\omega=2\pi/t'$ ($s\approx 0.075$) is the frequency resolution.

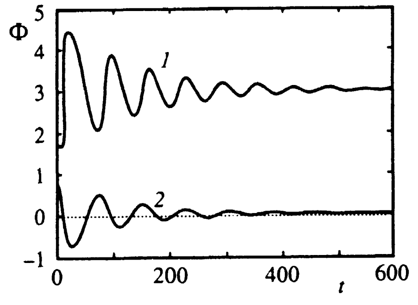

FIG. 2. Approach of $\Phi(t)$ to values corresponding to different fixed points $T=0.01$, $\nu=0.02$, and the values of the other parameters given in (3) for different initial conditions: $u(0)=0.62u_T$, $v(0)=1.232v_T$, $\Phi(0)=0.55\pi$ (curve *1*), and $\Phi(0)=0.25\pi$ (curve 2).

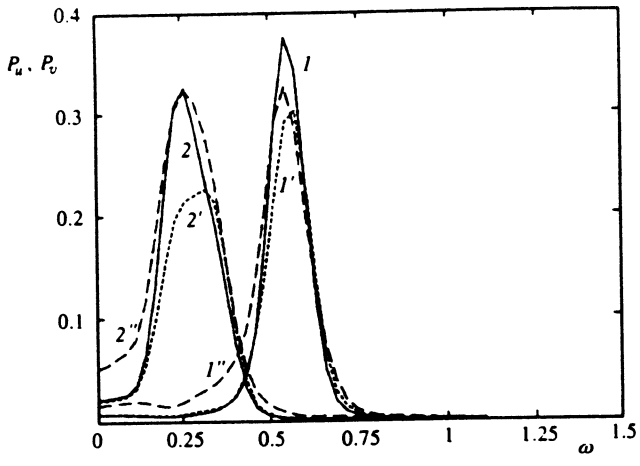

FIG. 3. Spectral densities $P_u(\omega)$ (curves *1*, *1'*, *1''*) and $P_v(\omega)$ (curves *2*, *2'*, *2''*) with $\sigma=0.0055$ and different values of the parameters: *1*,*2*—$T=0.01$, $\lambda=0.03$, $\nu=0.03$; *1'*,*2''*—$T=0.01$, $\lambda=0.05$, $\nu=0.0$; *1''*,*2''*—$T=0.015$, $\lambda=0.05$, $\nu=0$.

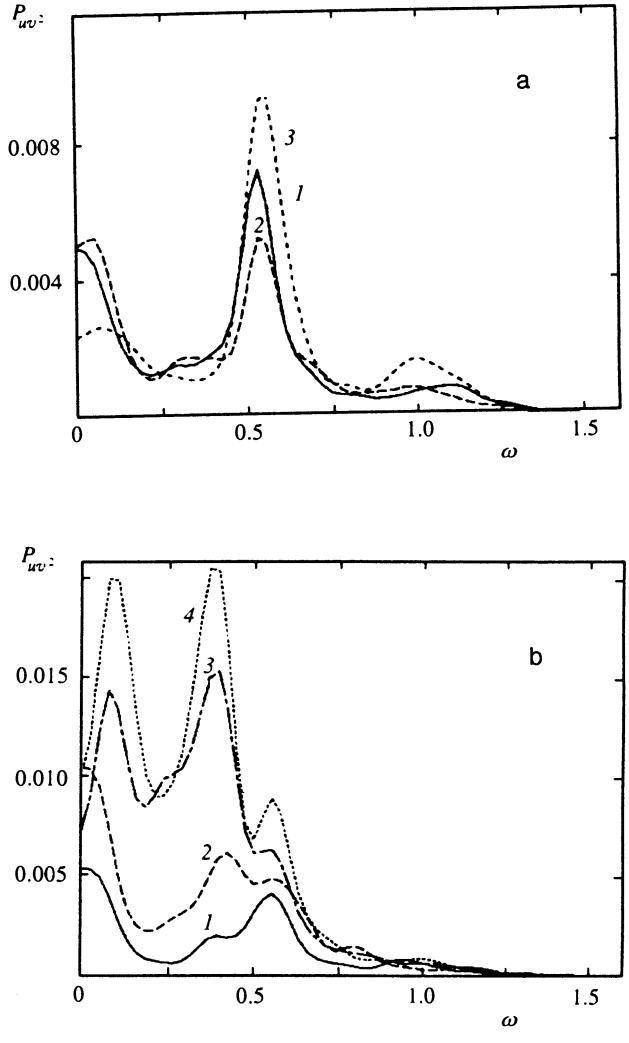

FIG. 4. Spectral density P_{uv^2} for $T=0.01$, $\sigma=0.0055$, $\lambda=0.03$, and $\nu=0.0$, 0.03, and 0.06 [curves *1–3*, respectively, (a)] and $\lambda=0.05$ and $\nu=0.0$, 0.04, 0.05, and 0.06 [curves *1–4*, respectively (b)].

5. COMPUTATIONAL RESULTS

Figure 3 displays the spectral density (spectral power) obtained for the realizations $u(t)$ and $v(t)$ by the above-described method for $Mt'=3500$ and the parameter values given in (3). During this time interval the spectral density reaches a stationary value and thereafter remains essentially constant. The function $P_u(\omega)$ is characterized by a broadened peak at the frequency ω_0; $P_v(\omega)$ contains, together with broadening, an appreciable low-frequency contribution, which indicates that slow processes occur in the system. The calculations show that these low-frequency contributions are virtually absent from $P_u(\omega)$.

As noted in Refs. 8 and 10, the most important indication of phase synchronization is the nontrivial character of the dynamics for $\omega \ll \omega_0$, specifically, the appearance of a "central peak" in the spectral density $P_{uv^2}(\omega)$. Indeed, at $\omega_0=2\Omega_0$ the quantity $u(t)v^2(t)$ must contain a contribution C which remains constant in the limit $t\to\infty$ and depends on the relative phase of the modes $u(t)$ and $v(t)$. In the phase synchronization regime, this phase is a determinate quantity (see Ref. 10), and for this reason it gives a contribution of the form $\bar{C}^2\delta(\omega)$ to $P_{uv^2}(\omega)$ on averaging over the random forces. Here, $|\bar{C}|\approx|\cos\Phi|\approx 1$ since the stationary values of Φ are close to 0 or π (see Sec. III). In the absence of phase synchronization, however, $\bar{C}=0$. This contribution also does not arise if the deviation from the resonance conditions is sufficiently large, when $\nu=\omega_0-2\Omega_0$ is not small ($\nu>\nu_c$). For $T=0.01$ and $\lambda=0.03$, this happens for $\omega_0=0.55$ and $\Omega_0=0.245$—compares the curves *1*, *2*, and *3* in Fig. 4. Errors in the numerical calculations, especially the finite size of the integration step, can lead to the appearance of a spurious central peak. We chose the step so that the central peak would be absent for selected values of σ and other parameters, when $\lambda=0$.

As one can see from the data shown in Fig. 4, the central peak exists over a wide range of ν. It should be noted that the spectral density peaks at $\omega\neq 0$. This indicates that slow quasiperiodic processes occur in the system. Direct observation of the trajectories $u(t)$ and $v(t)$ shows that these processes can be identified with transitions induced by thermal noise between the stable phase-synchronization points, where $u(t)$ and $v^2(t)$ oscillate approximately in phase or antiphase. This significant property is an important feature of the system of equations (2) and does not show up in the simplified model (4).

Comparing Figs. 4(a) and 4(b) shows that the behavior of the spectrum for large detunings ν (at the threshold where phase synchronization vanishes) is very sensitive to the values of the coupling constant λ. For $\lambda=0.05$ the "ordinary" beats with frequency ν and the above-discussed "nontrivial" low-frequency dynamics are superposed on one another, and this results in the appearance of two distinct peaks. For $\lambda=0.03$ these beats are less pronounced.

We now discuss the sensitivity of the results to the model parameters. As one can see from Figs. 5 and 6, phase synchronization appears more easily both as λ increases (which is quite natural) and as T increases. For a system in a heat bath (i.e., with white noise), this result is nontrivial and,

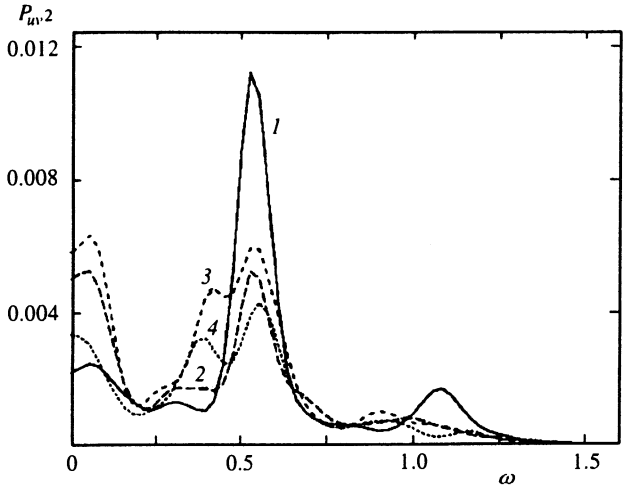

FIG. 5. Spectral density P_{uv}^2 for $T=0.01$, $\nu=0.03$, $\sigma=0.0055$, and $\lambda=0.01$, 0.03, 0.04, and 0.05 (curves *1–4*, respectively).

as far as we know, this is the first proof of its existence. Indeed, as T increases, not only do the equilibrium amplitudes u and v increase (this effect is understandable and reduces to an effective increase of λ), but both the damping and the noise intensity—factors whose role is very difficult to assess analytically—also increase.

The critical value of λ at which phase synchronization appears lies in the range 0.03–0.05 (for $T=0.01$). As we have already mentioned, phase synchronization appears more easily as the temperature increases. For large values of T (or λ with fixed T), wide-band noise (curve *5* in Fig. 6) appears in addition to the central peak in $P_{uv}^2(\omega)$; this probably indicates that the intermode pumping of energy, described by the term λuv^2 in Eq. (1), is chaotic. We do not possess sufficient data to choose an adequate scenario of the transition to chaos. At the same time, we note that this transition is

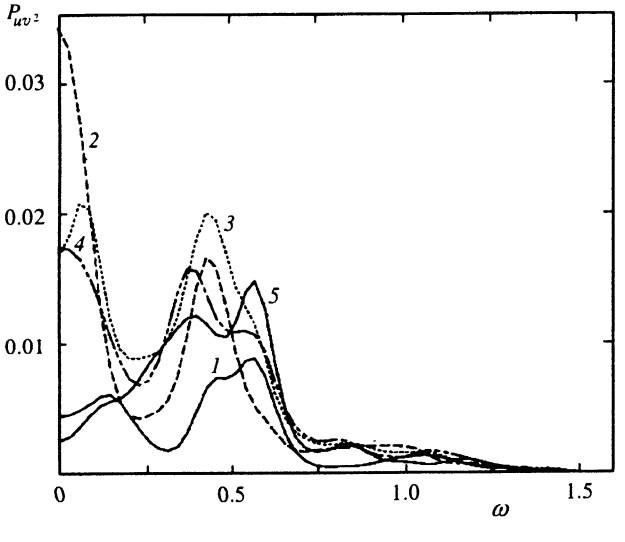

FIG. 6. Spectral density P_{uv}^2 for $\nu=0$, $\sigma=0.0055$, $\lambda=0.05$ and $T=0.01$ (curve *1*), $T=0.012$ (*2*), $T=0.014$ (*3*), $T=0.015$ (*4*), and $T=0.016$ (*5*).

accompanied by the appearance of additional peaks in $P_{uv}^2(\omega)$, indicating that the number of harmonics increases (see curves *4* and *5* in Fig. 3).

It should be noted that the critical values of T and λ for the transition to chaotic behavior are very sensitive to the choice of σ, and they decrease as σ decreases.

6. DISCUSSION OF RESULTS AND CONCLUSIONS

We now discuss the possible physical consequences of these results. As shown in Ref. 10, phase synchronization for phonons with $\mathbf{q}=\mathbf{q}_0$ should result in the appearance of waves of quasistatic displacements of atoms with this value of $\mathbf{q}$. We underscore the fact that this result cannot be obtained on the basis of the model (2) investigated here, since, as shown in Ref. 10, for quasistatic displacements to appear, transfer processes and the spatial dispersion of u and v must be taken into account explicitly and terms of the type uv^3 (intramode anharmonicity) must also be included in the Lagrangian (1). The term uv^3 has the effect of eliminating the phonon carrier frequency, and this is important for separating the contributions of quasistatic displacements. The amplitude of the quasistatic displacements is then found to be proportional to the height of the central peak in $P_{uv}^2(\omega)$.

The proof of the possibility of the appearance of quasistatic displacements, as discussed in Ref. 10, is quite rigorous in this section; the key problem is the appearance of phase synchronization itself. Moreover, phase synchronization should be manifested as splitting of the phonon frequencies for $\mathbf{q}=\mathbf{q}_0$ or, at least, as a sudden broadening of these peaks, if the resolution is high enough. The analysis of the experimental data performed in Ref. 10 seems to show that this behavior occurs in alkali metals for

$$\mathbf{q}_0=\frac{2\pi}{a}\left(\frac{2}{3},\frac{2}{3},\frac{2}{3},\frac{2}{3}\right),$$

but more accurate measurements are required in order to draw final conclusions.

Our results show that near room temperature T_r, alkali metals are suitable objects for observing phase synchronization. Appropriate experiments may be feasible (i.e., a search could be made for quasistatic "ω-like" displacements[10]) for $T_r<T<T_m$, where T_m is the melting point. An even better object is the high-temperature bcc phase of alkaline-earth metals (Ca and Sr), whose phonon spectra are similar to those of alkali metals and whose anharmonicity is much stronger.[20]

We also call attention to the newly discovered transition to chaotic phonon dynamics with increasing T (Fig. 6). It is possible that in metals, at least for certain modes, the phonon picture no longer provides a faithful representation near T_m, not only under conditions of very strong anharmonicity (as shown in Ref. 18) but also with moderate anharmonicity and a resonance ratio of the frequencies. By an unfaithful phonon picture we mean a situation in which the structure factor $S(\mathbf{q},\omega)$ at fixed $\mathbf{q}$ for a given polarization vector does not have a well defined (i.e., sufficiently narrow) peak as a function of ω, or it has more than one peak, so that the phonon frequency cannot be determined. This situation was dis-

cussed qualitatively in Ref. 7 in connection with the scenario of melting of alkali metals. An investigation of this situation in more realistic models (including the coordinate dependence of the displacements) is a very interesting problem. It is also of interest to describe in detail the transition to chaos in the model under study from a more formal point of view; this requires the use of more subtle and rigorous methods for solving the stochastic differential equations than the method used in Ref. 17.

In summary, the Fermi-resonance picture which we investigated (rational ratio of phonon frequencies) in the classical case, which is characteristic of metals, is much richer and more complicated than the ultraquantum limit typical of molecules consisting of light atoms.

The investigation described in the present paper was made possible by partial support provided by the International Science Foundation (Grant RGQ 000).

[1] H. Haken, *Advanced Synergetics: Instability Hierarchies of Self-Organizing Systems and Devices*, Springer-Verlag, New York (1983).
[2] H. G. Schuster, *Deterministic Chaos*, Physik-Verlag, VCH Publishers, Deerfield Beach, FL (1984).
[3] A. J. Lichtenberg and M. A. Lieberman, *Regular and Stochastic Motion*, Springer-Verlag, N. Y. (1983).
[4] R. Peierls, *Quantum Theory of Solids*, Clarendon Press, Oxford (1955).
[5] R. A. Cowley, Adv. Phys. **12**, 421 (1963).
[6] V. G. Vaks, S. P. Kravchuk, and A. V. Trefilov, J. Phys. F **10**, 2325 (1980).
[7] M. I. Katsnel'son and A. V. Trefilov, Fiz. Met. Metalloved. **64**, 629 (1987).
[8] M. I. Katsnel'son and A. V. Trefilov, JETP Lett. **45**, 634 (1987).
[9] P. W. Anderson, Phys. Rev. **109**, 1492 (1958).
[10] M. I. Katsnel'son and A. V. Trefilov, Zh. Éksp. Teor. Fiz. **97**, 1892 (1990) [Sov. Phys. JETP **70**, 1067 (1990)].
[11] B. P. Bak, T. Bohr, and M. H. Jensen, Phys. Scripta T **9**, 50 (1985).
[12] A. A. Vitt and G. S. Gorelik, Zh. Tekh. Fiz. **3**, 294 (1933).
[13] E. Fermi, Z. Phys. **71**, 250 (1931).
[14] A. Pippard, *The Physics of Vibration*, Cambridge University Press, N. Y. (1989).
[15] M. P. Lisitsa and A. M. Yaremko, *Fermi Resonance* [in Russian], Naukova dumka, Kiev, 1984.
[16] N. G. van Kampen, *Stochastic Processes in Physics and Chemistry*, North-Holland, N. Y. (1992).
[17] H. S. Greenside and E. Helfand, Bell Syst. Tech. J. **60**, 1927 (1981).
[18] Yu. N. Gornostyrev, M. I. Katsnel'son, and A. V. Trefilov, JETP Lett. **56**, 529 (1992).
[19] M. Takahashi, J. Phys. Soc. Jpn. **52**, 2592 (1983).
[20] V. G. Vaks, G. D. Samolyuk, and A. V. Trefilov, Phys. Lett. A **127**, 37 (1988).

Translated by M. E. Alferieff